

Agentic Hives: Equilibrium, Indeterminacy, and Endogenous Cycles in Self-Organizing Multi-Agent Systems

Jean-Philippe Garnier*

BrainiaK

Gap, France

February 2026

Abstract

Current multi-agent AI systems operate with a fixed number of agents whose roles are specified at design time. No formal theory governs when agents should be created, destroyed, or re-specialized at runtime—let alone how the population structure responds to changes in resources or objectives.

We introduce the *Agentic Hive*, a framework in which a variable population of autonomous micro-agents—each equipped with a sandboxed execution environment and access to a language model—undergoes *demographic dynamics*: birth, duplication, specialization, and death. Agent families play the role of production sectors, compute and memory play the role of factors of production, and an orchestrator plays the dual role of Walrasian auctioneer and Global Workspace.

Drawing on the multi-sector growth theory developed for dynamic general equilibrium (Benhabib & Nishimura, 1985; Venditti, 2005; Garnier, Nishimura & Venditti, 2013), we prove seven analytical results: (i) existence of a Hive Equilibrium via Brouwer’s fixed-point theorem; (ii) Pareto optimality of the equilibrium allocation; (iii) multiplicity of equilibria under strategic complementarities between agent families; (iv)–(v) Stolper–Samuelson and Rybczynski analogs that predict how the Hive restructures in response to preference and resource shocks; (vi) Hopf bifurcation generating endogenous demographic cycles; and (vii) a sufficient condition for local asymptotic stability.

The resulting *regime diagram* partitions the parameter space into regions of unique equilibrium, indeterminacy, endogenous cycles, and instability. Together with the comparative-statics matrices, it provides a formal governance toolkit that enables operators to predict and steer the demographic evolution of self-organizing multi-agent systems.

Keywords: multi-agent systems, general equilibrium, dynamic general equilibrium, agent demographics, indeterminacy, endogenous cycles, Hopf bifurcation, LLM orchestration.

*Corresponding author. E-mail: jeanphi@brainiak.ai.

Contents

| | | |
|----------|--|-----------|
| 1 | Introduction | 3 |
| 1.1 | The missing theory | 3 |
| 1.2 | Our approach | 3 |
| 1.3 | Contributions | 4 |
| 1.4 | Relation to prior work by the author | 4 |
| 2 | Related work | 5 |
| 3 | The Agentic Hive model | 5 |
| 3.1 | Agents, families, and resources | 5 |
| 3.2 | Production and externalities | 6 |
| 3.3 | Social welfare and the orchestrator’s problem | 7 |
| 3.4 | Population dynamics | 8 |
| 3.5 | Hive Equilibrium | 8 |
| 4 | Main results | 9 |
| 4.1 | Existence of Hive Equilibrium | 9 |
| 4.2 | Pareto optimality | 9 |
| 4.3 | Multiplicity and indeterminacy | 10 |
| 4.4 | Stolper–Samuelson analog | 11 |
| 4.5 | Rybczynski analog | 11 |
| 4.6 | Endogenous cycles | 12 |
| 4.7 | Stability conditions | 12 |
| 5 | Numerical illustrations | 13 |
| 5.1 | Three-family Hive ($S = 3, M = 2$) | 13 |
| 5.2 | Five-family Hive ($S = 5, M = 3$) | 15 |
| 6 | The regime diagram | 17 |
| 7 | Discussion | 18 |
| 7.1 | A macroeconomic governance framework | 18 |
| 7.2 | Connection to Global Workspace Theory | 18 |
| 7.3 | Imperfect information and mechanism design | 18 |
| 7.4 | Relation to evolutionary dynamics | 19 |
| 7.5 | Limitations | 19 |
| 8 | Conclusion | 20 |
| A | Proofs and technical details | 22 |
| A.1 | Proof details for Theorem 4.4 (Multiplicity) | 22 |
| A.2 | Proof details for Theorem 4.6 (Stolper–Samuelson) | 23 |
| A.3 | Proof details for Theorem 4.10 (Endogenous cycles) | 23 |
| A.4 | Lyapunov property and welfare monotonicity | 24 |

1 Introduction

The past two years have witnessed an explosion of multi-agent systems built around large language models (LLMs). Systems such as AutoGen [29], CrewAI [5], MetaGPT [14], and Swarm [24] enable several LLM-powered agents to collaborate on complex tasks.

All of these systems share a common architectural assumption: *the number of agents is fixed at design time, and their roles are pre-assigned*. The system designer decides that there will be a “planner” agent, a “coder” agent, and a “reviewer” agent, then hard-codes the interaction protocol. If the task mix changes, or if resources become scarce, or if one agent family becomes redundant, the system has no principled mechanism for adaptation.

This is the equivalent of running an economy without a theory of growth: you can allocate resources across existing firms, but you have no formal basis for deciding when new firms should enter, when existing ones should exit, or how the industrial structure should respond to a technology shock.

1.1 The missing theory

We argue that the missing ingredient is a *macroeconomic theory of agent demographics*. Specifically, we need formal answers to four questions:

(Q1) **Entry:** When should new agents be created, and of what type?

(Q2) **Exit:** When should existing agents be removed?

(Q3) **Specialization:** How should undifferentiated agents acquire functional roles?

(Q4) **Restructuring:** How does the entire population structure respond to changes in resources or objectives?

No existing framework provides analytical answers to (Q1)–(Q4). Swarm intelligence [7, 18] studies self-organization but provides no equilibrium theory. Multi-agent reinforcement learning (MARL) [19] learns policies but does not model population dynamics. Agent-based computational economics (ACE) [26] simulates agent populations but offers no closed-form results.

1.2 Our approach

We observe that (Q1)–(Q4) are *precisely* the questions addressed by the theory of multi-sector economic growth—a branch of dynamic general equilibrium theory that has been developed over seven decades, from Arrow & Debreu [1], Debreu [4], and McKenzie [20] to Garnier, Nishimura & Venditti [10].

The mapping is direct:

| Multi-sector economy | Agentic Hive |
|------------------------------|---|
| Production sectors | Agent families (perception, planning, ...) |
| Factors (capital, labor) | Resources (GPU, memory, attention, ...) |
| Output of sector j | Task completion by family j |
| Factor prices | Shadow prices of resources |
| Consumer preferences | System objectives (quality, cost, latency, ...) |
| Walrasian auctioneer | Orchestrator / Global Workspace |
| Inter-sectoral externalities | Cross-family spillovers |
| Steady-state population | Hive Equilibrium |

This is not a metaphor. As we show formally in Section 3, the mathematical objects are identical: the population dynamics of agent families are governed by a dynamical system whose steady states are general equilibria, whose comparative statics obey Stolper–Samuelson and Rybczynski theorems, and whose stability properties determine the existence of endogenous demographic cycles.

1.3 Contributions

We introduce the *Agentic Hive*, a formal framework for self-organizing multi-agent systems with variable population, and establish the following results:

1. **Existence** (Theorem 4.1): Under standard regularity assumptions, at least one Hive Equilibrium exists.
2. **Pareto optimality** (Theorem 4.2): Every Hive Equilibrium is Pareto-optimal when the orchestrator has full information.
3. **Multiplicity** (Theorem 4.4): Under strategic complementarities between agent families, multiple equilibria coexist—corresponding to distinct “morphologies” of the Hive.
4. **Stolper–Samuelson analog** (Theorem 4.6): A magnification effect links preference changes to resource price changes.
5. **Rybczynski analog** (Theorem 4.8): A magnification effect links resource endowment changes to population restructuring.
6. **Endogenous cycles** (Theorem 4.10): A Hopf bifurcation generates periodic demographic oscillations—the “seasons” of the Hive.
7. **Stability** (Theorem 4.12): A sufficient condition on mortality rates guarantees local asymptotic stability.

Together, these results yield a *regime diagram* (Section 6) that partitions the parameter space into regions of qualitatively distinct behavior, providing a formal governance toolkit for designers and operators of multi-agent systems.

1.4 Relation to prior work by the author

The author’s doctoral work [9, 10] characterized local indeterminacy in continuous-time multi-sector growth models, establishing conditions under which competitive equilibrium cycles arise from the interaction of returns to scale and consumer preferences. The present paper transports this toolkit to the entirely different domain of multi-agent AI systems,

extending it from fixed-population general equilibrium to variable populations with endogenous demographics and multi-regime dynamics.

2 Related work

Multi-agent LLM systems. AutoGen [29], MetaGPT [14], CrewAI [5], and Swarm [24] enable multi-agent collaboration with LLMs. All assume a fixed agent set with pre-defined roles. Recent surveys [12] catalog the rapid growth of this field but do not identify population dynamics as a research gap.

Swarm intelligence. Ant Colony Optimization [7], Particle Swarm Optimization [18], and related algorithms use local interaction rules to achieve collective behavior. These approaches do not provide equilibrium concepts, comparative statics, or stability theorems.

Evolutionary game theory. The replicator equation [13] governs population shares under frequency-dependent fitness. Our population dynamics (Section 3.4) are a generalization of replicator dynamics to absolute populations with endogenous resource allocation and multi-sector externalities.

Agent-based computational economics. ACE [26] simulates heterogeneous agent populations but produces no closed-form results. Our framework provides analytical theorems that complement simulation.

Multi-sector growth theory. Benhabib & Nishimura [3] established the existence of competitive equilibrium cycles in multi-sector optimal growth models. Venditti [28] and Garnier, Nishimura & Venditti [10] extended these results to characterize indeterminacy under various assumptions on returns to scale and preferences. We transport this entire toolkit to agent demographics.

Global Workspace Theory. Baars [2] proposed that consciousness arises from a global workspace that integrates and broadcasts information from specialist processors. Our orchestrator plays an analogous role: it selects, integrates, and broadcasts resource allocation signals across agent families.

3 The Agentic Hive model

3.1 Agents, families, and resources

Definition 3.1 (Agentic Hive). An *Agentic Hive* is a tuple $\mathcal{H} = (\mathcal{A}_t, \mathcal{F}, \mathbf{R}, \mathbf{w}, \Gamma, \Theta)$ where:

- \mathcal{A}_t is the set of agents alive at time t , with $|\mathcal{A}_t| = N_{\text{total}}(t)$ variable;
- $\mathcal{F} = \{1, \dots, S\}$ is a finite set of *agent families* (functional specializations);
- $\mathbf{R} = (R^1, \dots, R^M) \in \mathbb{R}_+^M$ is the vector of resource endowments;
- $\mathbf{w} = (w_1, \dots, w_S) \in \Delta_S$ is the vector of global preferences over family outputs;
- $\Gamma = (\gamma_{jk})_{j,k} \in \mathbb{R}^{S \times S}$ is the externality matrix;

- Θ is the orchestrator.

We denote by $N_t^j \in \mathbb{R}_+$ the population of family j at time t , and by $\mathbf{N}_t = (N_t^1, \dots, N_t^S) \in \mathbb{R}_+^S$ the population vector.

Definition 3.2 (Agent). An agent $a \in \mathcal{A}_t$ is a tuple $a = (g_a, \sigma_a, f_a, \mu_a, \tau_a, \omega_a, \zeta_a)$ where:

- $g_a \in \mathcal{G}$: genome (base prompt, policy, configuration);
- $\sigma_a \in \Sigma$: internal state (local memory, context);
- $f_a \in \mathcal{F} \cup \{\emptyset\}$: family assignment (\emptyset for stem agents);
- $\mu_a \in \mathbb{R}_+^K$: performance profile (K metrics);
- $\tau_a \in \mathbb{R}_+$: age;
- ω_a : sandboxed execution environment;
- $\zeta_a \in [0, 1]$: degree of specialization (0 = totipotent, 1 = fully specialized).

Definition 3.3 (Stem agent). An agent a is a *stem agent* if $\zeta_a = 0$ and $f_a = \emptyset$. A stem agent can *duplicate* (create a copy with reset state) or *specialize* (transition to a family $j \in \mathcal{F}$ with $\zeta_a > 0$).

Resources are organized into M types. Each agent in family j consumes a resource vector; the aggregate consumption by family j of resource m is denoted K_j^m . The matrix $\mathbf{K} = (K_j^m)_{j,m} \in \mathbb{R}_+^{S \times M}$ records the full resource allocation.

Assumption 1 (Budget). Total population is bounded by a budget constraint: $\sum_{j=1}^S c_j N^j \leq B$, where $c_j > 0$ is the per-agent maintenance cost of family j and $B > 0$ is the total budget.

Define the *feasible population set*:

$$\Omega = \left\{ \mathbf{N} \in \mathbb{R}_+^S : \sum_{j=1}^S c_j N^j \leq B \right\}. \quad (1)$$

Ω is compact and convex.

3.2 Production and externalities

Each family produces output that depends on its resource allocation, its population, and spillovers from other families.

Definition 3.4 (Sectoral production). The output of family j is:

$$Y_j(\mathbf{K}_j, N^j, \mathbf{N}_{-j}) = A_j \cdot F_j(\mathbf{K}_j) \cdot (N^j)^{\eta_j} \cdot \Gamma_j(\mathbf{N}_{-j}), \quad (2)$$

where:

- $A_j > 0$ is the total factor productivity of family j ;
- $F_j : \mathbb{R}_+^M \rightarrow \mathbb{R}_+$ is a CES production function in resources:

$$F_j(\mathbf{K}_j) = \left[\sum_{m=1}^M \alpha_{jm} \left(K_j^m \right)^{\frac{\rho_j - 1}{\rho_j}} \right]^{\frac{\rho_j}{\rho_j - 1}}, \quad (3)$$

with $\alpha_{jm} > 0$, $\sum_m \alpha_{jm} = 1$, and $\rho_j > 0$ the elasticity of substitution;

- $(N^j)^{\eta_j}$ captures returns to scale within the family, with $\eta_j > 0$;
- $\Gamma_j(\mathbf{N}_{-j}) = \prod_{k \neq j} (N^k)^{\gamma_{jk}}$ is the externality term, with $\gamma_{jk} \in \mathbb{R}$.

Assumption 2 (Production regularity). For each j : (i) F_j is C^2 , increasing, and strictly concave; (ii) Inada conditions hold: $\partial F_j / \partial K_j^m \rightarrow \infty$ as $K_j^m \rightarrow 0^+$ and $\partial F_j / \partial K_j^m \rightarrow 0$ as $K_j^m \rightarrow \infty$; (iii) $0 < \eta_j < 1$ (decreasing returns within family; relaxed to $\eta_j \geq 1$ in Section 4.3).

Remark 3.5. The assumption $\eta_j < 1$ guarantees that the marginal value of an additional agent diminishes within each family, ensuring interior equilibria. In Theorem 4.4, we relax this to $\eta_j \geq 1$ for some families, which is the source of indeterminacy.

The externality matrix $E = (\gamma_{jk})$ is the central structural object of the theory:

- $\gamma_{jk} > 0$: family k generates a positive spillover on family j (complementarity);
- $\gamma_{jk} < 0$: family k imposes a negative externality on family j (congestion);
- $\gamma_{jk} = 0$: independence.

3.3 Social welfare and the orchestrator's problem

Definition 3.6 (Social welfare). The social welfare function is:

$$W(\mathbf{K}, \mathbf{N}) = \sum_{j=1}^S w_j \cdot u(Y_j(\mathbf{K}_j, N^j, \mathbf{N}_{-j})) - \sum_{j=1}^S c_j N^j, \quad (4)$$

where $u : \mathbb{R}_+ \rightarrow \mathbb{R}$ is a CRRA utility: $u(Y) = Y^{1-\sigma}/(1-\sigma)$ for $\sigma > 0$, $\sigma \neq 1$, and $u(Y) = \ln Y$ for $\sigma = 1$.

Definition 3.7 (Orchestrator's problem). Given population \mathbf{N} , the orchestrator solves the *inner problem*:

$$W^*(\mathbf{N}) = \max_{\mathbf{K} \geq 0} W(\mathbf{K}, \mathbf{N}) \quad \text{s.t.} \quad \sum_{j=1}^S K_j^m \leq R^m \quad \forall m \in \{1, \dots, M\}. \quad (5)$$

Assumption 3 (Utility regularity). u is C^2 , strictly increasing, and strictly concave on \mathbb{R}_{++} .

Assumption 4 (Weak externalities). The externality matrix satisfies

$$\|E\|_\infty = \max_j \sum_{k \neq j} |\gamma_{jk}| < \frac{1 - \eta_{\max}}{1 + \sigma \eta_{\max}}, \quad (6)$$

where $\eta_{\max} = \max_j \eta_j < 1$ (from Assumption 2(iii)) and σ is the CRRA parameter.

Remark 3.8. Assumption 4 ensures that the value function $W^*(\mathbf{N})$ is globally concave on Ω . The bound arises because the Hessian of W^* with respect to \mathbf{N} has diagonal terms of order $\eta_j - 1 < 0$ (diminishing returns) and off-diagonal terms of order γ_{jk} (externalities). Concavity holds when the negative diagonal dominates the off-diagonal perturbation. This assumption is relaxed in Section 4.3 to obtain indeterminacy.

Under Assumptions 2 and 3, the inner problem (5) has a unique solution $\mathbf{K}^*(\mathbf{N}) = (K_j^{m*}(\mathbf{N}))_{j,m}$, with associated shadow prices $\boldsymbol{\lambda}^*(\mathbf{N}) = (\lambda^{1*}, \dots, \lambda^{M*})$ satisfying the first-

order conditions:

$$w_j u'(Y_j^*) \cdot A_j \frac{\partial F_j}{\partial K_j^m} \Big|_{\mathbf{K}^*} \cdot (N^j)^{\eta_j} \Gamma_j = \lambda^{m*} \quad \forall j, m. \quad (7)$$

Definition 3.9 (Marginal social value). The marginal social value of an agent in family j is:

$$V_j(\mathbf{N}) = \frac{dW^*}{dN^j} = w_j u'(Y_j^*) \cdot \frac{\partial Y_j}{\partial N^j} \Big|_{\mathbf{K}^*} - c_j, \quad (8)$$

where the equality follows from the envelope theorem (the terms involving $\partial \mathbf{K}^* / \partial N^j$ vanish at the optimum).

Explicitly:

$$V_j(\mathbf{N}) = w_j u'(Y_j^*) \cdot A_j F_j(\mathbf{K}_j^*) \eta_j (N^j)^{\eta_j-1} \Gamma_j(\mathbf{N}_{-j}) - c_j. \quad (9)$$

3.4 Population dynamics

The demographic dynamics of the Hive are governed by a system of ODEs:

Definition 3.10 (Population dynamics). The population of family j evolves according to:

$$\frac{dN^j}{dt} = \Phi_j(\mathbf{N}) = V_j(\mathbf{N}) \cdot N^j, \quad j = 1, \dots, S. \quad (10)$$

This is a *selection dynamic* [13]: families with positive marginal value ($V_j > 0$) grow; families with negative marginal value ($V_j < 0$) decline.

In vector form: $\dot{\mathbf{N}} = \Phi(\mathbf{N})$, where $\Phi : \mathbb{R}_+^S \rightarrow \mathbb{R}^S$.

Remark 3.11 (Interpretation of V_j). The marginal social value V_j aggregates three forces:

- (i) *Direct returns*: an additional agent in family j increases Y_j through the term $(N^j)^{\eta_j}$;
- (ii) *Externalities*: through $\Gamma_j(\mathbf{N}_{-j})$, the output of family j depends on the populations of other families;
- (iii) *Cost*: the maintenance cost c_j reduces V_j .

When $V_j = 0$, family j is at demographic equilibrium: the marginal benefit of an additional agent exactly equals its cost.

Remark 3.12 (Relation to replicator dynamics). Equation (10) is a generalization of the replicator equation to absolute populations with endogenous fitness. In the classical replicator equation, $\dot{x}_i = x_i(f_i - f)$ with exogenous fitness f_i . Here, the “fitness” $V_j(\mathbf{N})$ is endogenous: it depends on all populations through the production functions, externalities, and the orchestrator’s optimal allocation.

3.5 Hive Equilibrium

Definition 3.13 (Hive Equilibrium). A *Hive Equilibrium* is a triple $(\mathbf{N}^*, \mathbf{K}^*, \boldsymbol{\lambda}^*)$ such that:

- (HE-1) **Allocation optimality**: \mathbf{K}^* solves the inner problem (5) for \mathbf{N}^* , with shadow prices $\boldsymbol{\lambda}^*$;

(HE-2) **Demographic stationarity:** $\Phi(\mathbf{N}^*) = 0$, i.e., for each j :

$$V_j(\mathbf{N}^*) = 0 \quad \text{if } N^{j*} > 0, \quad V_j(\mathbf{N}^*) \leq 0 \quad \text{if } N^{j*} = 0; \quad (11)$$

(HE-3) **Budget feasibility:** $\sum_j c_j N^{j*} \leq B$.

Condition (HE-2) states that at equilibrium, every active family has zero marginal social value (marginal benefit equals marginal cost), and no inactive family would be profitable if activated. This is the free-entry condition of competitive equilibrium theory.

4 Main results

4.1 Existence of Hive Equilibrium

Theorem 4.1 (Existence). *Under Assumptions 1–3, there exists at least one Hive Equilibrium $(\mathbf{N}^*, \mathbf{K}^*, \boldsymbol{\lambda}^*)$ with $\mathbf{N}^* \in \Omega$.*

Proof. For $\varepsilon > 0$ sufficiently small, define the truncated feasible set $\Omega_\varepsilon = \{\mathbf{N} \in \Omega : N^j \geq \varepsilon \forall j\}$, which is compact and convex.

Define the map $\Psi_\varepsilon : \Omega_\varepsilon \rightarrow \Omega_\varepsilon$ by:

$$\Psi_\varepsilon(\mathbf{N}) = \text{proj}_{\Omega_\varepsilon}(\mathbf{N} + \varepsilon \Phi(\mathbf{N})),$$

where $\text{proj}_{\Omega_\varepsilon}$ is the Euclidean projection onto Ω_ε .

Under our assumptions, $V_j(\mathbf{N})$ is continuous on Ω_ε (composition of C^2 functions), so Φ is continuous. The projection onto a closed convex set is continuous. Hence Ψ_ε is a continuous map from the compact convex set Ω_ε into itself.

By Brouwer's fixed-point theorem, Ψ_ε has a fixed point \mathbf{N}_ε^* .

Taking a convergent subsequence as $\varepsilon \rightarrow 0$ (by compactness of Ω), the limit $\mathbf{N}^* \in \Omega$ satisfies $\Phi(\mathbf{N}^*) = 0$ at interior components and $V_j(\mathbf{N}^*) \leq 0$ at boundary components ($N^{j*} = 0$).

The allocation \mathbf{K}^* and prices $\boldsymbol{\lambda}^*$ are obtained from the inner problem at \mathbf{N}^* . \square

4.2 Pareto optimality

Theorem 4.2 (First Welfare Theorem for Hives). *Under Assumptions 1–4, every Hive Equilibrium $(\mathbf{N}^*, \mathbf{K}^*, \boldsymbol{\lambda}^*)$ is Pareto-optimal: there exists no feasible $(\mathbf{N}', \mathbf{K}')$ with $W(\mathbf{K}', \mathbf{N}') > W(\mathbf{K}^*, \mathbf{N}^*)$.*

Proof. At a Hive Equilibrium, \mathbf{K}^* maximizes $W(\cdot, \mathbf{N}^*)$ over resource constraints (HE-1), and \mathbf{N}^* satisfies $V_j(\mathbf{N}^*) = dW^*/dN^j = 0$ for all active families (HE-2).

Suppose for contradiction that there exists feasible $(\mathbf{N}', \mathbf{K}')$ with $W(\mathbf{K}', \mathbf{N}') > W(\mathbf{K}^*, \mathbf{N}^*)$.

Since $W^*(\mathbf{N}) = \max_{\mathbf{K}} W(\mathbf{K}, \mathbf{N})$, we have $W^*(\mathbf{N}') \geq W(\mathbf{K}', \mathbf{N}') > W(\mathbf{K}^*, \mathbf{N}^*) = W^*(\mathbf{N}^*)$.

We show that W^* is strictly concave in \mathbf{N} on Ω . The Hessian $H = D_{\mathbf{N}}^2 W^*$ has diagonal entries $H_{jj} = w_j [u''(Y_j^*) (\partial Y_j / \partial N^j)^2 + u'(Y_j^*) \partial^2 Y_j / (\partial N^j)^2]$, which are negative under Assumptions 2(iii) and 3 (the dominant term is $\eta_j(\eta_j - 1)(N^j)^{\eta_j - 2} < 0$). The off-diagonal

entries H_{jk} are bounded by a term proportional to $|\gamma_{jk}|$. By a Gershgorin argument on H , Assumption 4 ensures that every eigenvalue of H is strictly negative, so W^* is strictly concave on Ω .

The condition $\nabla_{\mathbf{N}} W^*(\mathbf{N}^*) = 0$ (from HE-2) then implies \mathbf{N}^* is the unique global maximum of W^* on Ω , contradicting $W^*(\mathbf{N}') > W^*(\mathbf{N}^*)$. \square

Remark 4.3. Pareto optimality relies on the orchestrator having *full information* about production functions and externalities. If some externalities are unobserved, the equilibrium may fail to be Pareto-optimal, necessitating Pigouvian corrections (see Section 7).

4.3 Multiplicity and indeterminacy

We now relax Assumptions 2(iii) and 4 to allow increasing returns for some families.

Assumption 5 (Strategic complementarity). There exist families j, k with $\gamma_{jk} > 0$ and $\gamma_{kj} > 0$ (mutual positive externalities).

Assumption 6 (Local increasing returns). There exists a family j_0 with $\eta_{j_0} \geq 1$ (non-decreasing returns within family).

Theorem 4.4 (Multiplicity of equilibria). *Under Assumptions 1–3, 5, and 6, there exist open sets of parameters (\mathbf{w}, \mathbf{R}) for which at least two distinct Hive Equilibria coexist.*

Proof sketch. Consider the simplest non-trivial case: $S = 2$ families with mutual complementarity ($\gamma_{12}, \gamma_{21} > 0$) and increasing returns for family 1 ($\eta_1 \geq 1$).

At a Hive Equilibrium, the active families satisfy $V_j(\mathbf{N}^*) = 0$, which defines two curves in (N^1, N^2) -space:

$$\mathcal{C}_1 = \{(N^1, N^2) : V_1(N^1, N^2) = 0\}, \quad \mathcal{C}_2 = \{(N^1, N^2) : V_2(N^1, N^2) = 0\}.$$

With increasing returns ($\eta_1 \geq 1$), \mathcal{C}_1 is non-monotone: V_1 increases with N^1 for small N^1 (increasing returns dominate) and decreases for large N^1 (resource scarcity dominates). With positive externalities ($\gamma_{12} > 0$), V_1 increases with N^2 , tilting \mathcal{C}_1 in (N^1, N^2) -space.

For sufficiently strong complementarities, \mathcal{C}_1 and \mathcal{C}_2 intersect at least twice, yielding at least two interior equilibria with distinct population structures.

Full details, including the computation of the crossing conditions, are given in Appendix A. \square

Remark 4.5 (Interpretation). The multiple equilibria correspond to distinct “morphologies” of the Hive:

- *Exploitation equilibrium*: high specialization, concentrated populations, high efficiency;
- *Exploration equilibrium*: high diversity, distributed populations, robustness to perturbation.

The system can settle into either morphology depending on initial conditions and historical path—a form of *path dependence* directly analogous to the indeterminacy in multi-sector growth models [3, 10].

4.4 Stolper–Samuelson analog

Theorem 4.6 (Hive Stolper–Samuelson). *At an interior Hive Equilibrium, the Jacobian matrix*

$$\mathbf{SS} = \frac{\partial \boldsymbol{\lambda}^*}{\partial \mathbf{w}} \in \mathbb{R}^{M \times S} \quad (12)$$

satisfies a magnification effect: if preference w_j increases (ceteris paribus), the shadow price λ^{m} of the resource most intensively used by family j increases proportionally more than the preference change:*

$$\frac{\hat{\lambda}^{m*}}{\hat{w}_j} > 1 \quad \text{for the resource } m \text{ used most intensively by family } j, \quad (13)$$

where $\hat{x} = dx/x$ denotes a proportional change.

Proof sketch. Differentiate the first-order conditions (7) totally with respect to \mathbf{w} . The resulting linear system, combined with the resource constraints $\sum_j K_j^{m*} = R^m$ and the CES structure of F_j , yields the Stolper–Samuelson matrix whose structure is inherited from the factor intensity matrix $\boldsymbol{\theta} = (\theta_{jm})$ with $\theta_{jm} = \lambda^{m*} K_j^{m*} / (w_j u'(Y_j^*) Y_j^*)$.

The magnification effect follows from the algebraic structure of $\boldsymbol{\theta}^{-1}$ when $S = M$, and from generalized Stolper–Samuelson results [16, 8] when $S \neq M$. See Appendix A. \square

Remark 4.7 (Operational interpretation). Suppose the system administrator increases the weight on quality ($w_{\text{qual}} \uparrow$). The SS matrix predicts which resources will become scarce (e.g., GPU if quality-intensive families are GPU-heavy) *before the change is applied*. This is a *predictive governance* tool: the operator can anticipate bottlenecks and provision resources accordingly.

4.5 Rybczynski analog

Theorem 4.8 (Hive Rybczynski). *At an interior Hive Equilibrium, the Jacobian matrix*

$$\mathbf{RB} = \frac{\partial \mathbf{N}^*}{\partial \mathbf{R}} \in \mathbb{R}^{S \times M} \quad (14)$$

satisfies a magnification effect: if endowment R^m increases (ceteris paribus), the equilibrium population of the family that uses resource m most intensively expands proportionally more than the endowment change, while other families may contract:

$$\frac{\hat{N}^{j*}}{\hat{R}^m} \begin{cases} > 1 & \text{if family } j \text{ uses } m \text{ most intensively,} \\ < 0 & \text{for some families } j' \neq j. \end{cases} \quad (15)$$

Proof sketch. At steady state, $\Phi(\mathbf{N}^*, \mathbf{R}) = 0$. By the implicit function theorem (assuming $D_{\mathbf{N}}\Phi$ is non-singular):

$$\frac{\partial \mathbf{N}^*}{\partial \mathbf{R}} = -\left(D_{\mathbf{N}}\Phi\right)^{-1} D_{\mathbf{R}}\Phi.$$

The structure of $D_{\mathbf{R}}\Phi$ reflects how resource changes affect marginal values V_j through the allocation $\mathbf{K}^*(\mathbf{N}, \mathbf{R})$. The magnification effect follows from the factor intensity structure, as in the classical Rybczynski theorem. See Appendix A. \square

Remark 4.9 (Operational interpretation). Suppose a second GPU cluster is added to the system ($R^{\text{gpu}} \uparrow$). The RB matrix predicts that GPU-intensive families (e.g., generation, transformation) will *proliferate*, while CPU-light families (e.g., logging, monitoring) may *decline*—not because they are less useful, but because the system re-optimizes the allocation. This is a *capacity planning theorem*: the operator can predict how the Hive will restructure before provisioning hardware.

4.6 Endogenous cycles

Theorem 4.10 (Endogenous demographic cycles). *Under Assumptions 1–3 and 5, suppose that:*

- (i) $S \geq 2$;
- (ii) *The Jacobian $J = D_{\mathbf{N}}\Phi(\mathbf{N}^*)$ at an interior Hive Equilibrium \mathbf{N}^* has a pair of complex conjugate eigenvalues $\alpha(p) \pm i\beta(p)$, where p is a bifurcation parameter (e.g., an externality strength γ_{jk});*
- (iii) **Transversality:** $d\alpha/dp|_{p=p_0} \neq 0$ at the value p_0 where $\alpha(p_0) = 0$;
- (iv) *All other eigenvalues of J have strictly negative real parts at p_0 .*

Then a Hopf bifurcation occurs at $p = p_0$: for p near p_0 , a family of periodic orbits (limit cycles) bifurcates from the equilibrium \mathbf{N}^ .*

Proof. This is a direct application of the Hopf bifurcation theorem [21, 11] to the system $\dot{\mathbf{N}} = \Phi(\mathbf{N}; p)$. Conditions (i)–(iv) are exactly the hypotheses of the theorem.

It remains to verify that these conditions can be satisfied for some parameter configuration. This is demonstrated by construction in Appendix A, where we exhibit a two-family example with explicit parameter values yielding complex eigenvalues crossing the imaginary axis. \square

Remark 4.11 (The “seasons” of the Hive). The periodic orbits generated by the Hopf bifurcation correspond to cyclical phases of the Hive’s demographic structure:

- *Expansion phase:* births exceed deaths, population grows, new agents explore diverse tasks;
- *Consolidation phase:* successful families specialize, efficiency increases, diversity decreases;
- *Contraction phase:* deaths exceed births, underperforming agents are pruned, resources are freed;
- *Renewal phase:* stem agents regenerate diversity, the cycle restarts.

These cycles are *endogenous*—driven by the internal dynamics of externalities and returns to scale, not by external shocks. This is the agent-demographic analog of the competitive equilibrium cycles of Benhabib & Nishimura [3].

4.7 Stability conditions

Theorem 4.12 (Local stability). *An interior Hive Equilibrium \mathbf{N}^* is locally asymptotically stable if and only if all eigenvalues of the Jacobian $J = D_{\mathbf{N}}\Phi(\mathbf{N}^*)$ have strictly*

negative real parts.

A sufficient condition is:

$$\eta_{\max} < 1 \quad \text{and} \quad \|E\|_{\infty} \cdot \max_j N^{j*} < \min_j |V'_j(\mathbf{N}^*)| \cdot N^{j*}, \quad (16)$$

where $\eta_{\max} = \max_j \eta_j$ and $\|E\|_{\infty}$ is the infinity norm of the externality matrix.

Proof. The Jacobian at an interior equilibrium ($V_j(\mathbf{N}^*) = 0$) is:

$$J_{jk} = \left. \frac{\partial \Phi_j}{\partial N^k} \right|_{\mathbf{N}^*} = \left. \frac{\partial V_j}{\partial N^k} \right|_{\mathbf{N}^*} \cdot N^{j*} + V_j(\mathbf{N}^*) \cdot \delta_{jk} = \left. \frac{\partial V_j}{\partial N^k} \right|_{\mathbf{N}^*} \cdot N^{j*}, \quad (17)$$

since $V_j(\mathbf{N}^*) = 0$. Thus $J = \text{diag}(\mathbf{N}^*) \cdot D_{\mathbf{N}}V(\mathbf{N}^*)$.

The diagonal terms are $J_{jj} = (\partial V_j / \partial N^j) \cdot N^{j*}$. Under $\eta_j < 1$, $\partial V_j / \partial N^j < 0$ (diminishing returns), so $J_{jj} < 0$.

The off-diagonal terms are $J_{jk} = (\partial V_j / \partial N^k) \cdot N^{j*}$, whose sign is determined by the externality γ_{jk} .

By the Gershgorin circle theorem, all eigenvalues of J lie in the union of disks centered at J_{jj} with radius $\sum_{k \neq j} |J_{jk}|$. The sufficient condition (16) ensures that these disks lie entirely in the left half-plane. \square

Remark 4.13 (Governance lever). The stability condition can be interpreted as a requirement that the “mortality pressure” (captured by $|V'_j| \cdot N^{j*}$, the speed at which declining families shrink) dominates the “amplification pressure” from cross-family externalities ($\|E\|_{\infty} \cdot N^{j*}$). The orchestrator can enforce stability by increasing the sensitivity of the birth-death mechanism to marginal value deviations.

5 Numerical illustrations

We complement the analytical results with numerical computations for $S = 3$ and $S = 5$ families, illustrating the equilibrium structure, regime transitions, and dynamic behavior predicted by the theory. All computations use log utility ($\sigma = 1$) and CES production with the parameters specified below.

5.1 Three-family Hive ($S = 3$, $M = 2$)

Consider three agent families—*perception* ($j = 1$), *reasoning* ($j = 2$), and *generation* ($j = 3$)—sharing two resources: GPU ($m = 1$) and memory ($m = 2$).

Parameters. $A_j = 1$ for all j ; $c_j = 1$; $B = 15$; $R^1 = 10$ (GPU), $R^2 = 8$ (memory). CES elasticities: $\rho_1 = 0.8$, $\rho_2 = 1.2$, $\rho_3 = 0.6$. Factor shares: $\alpha_1 = (0.3, 0.7)$ (memory-intensive), $\alpha_2 = (0.5, 0.5)$ (balanced), $\alpha_3 = (0.8, 0.2)$ (GPU-intensive). Preferences: $\mathbf{w} = (0.35, 0.40, 0.25)$.

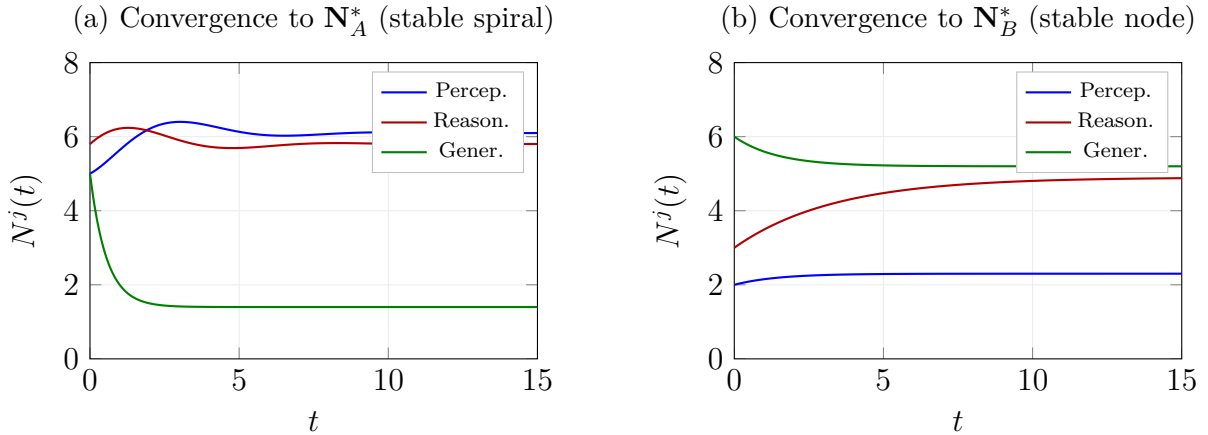


Figure 1: Path dependence in the three-family Hive ($S = 3$, $M = 2$) with $\eta_1 = 1.3$ and $\gamma_{12} = \gamma_{21} = 0.4$. **(a)** From $\mathbf{N}_0 = (5.0, 5.0, 5.0)$, the system spirals into the perception-dominant morphology $\mathbf{N}_A^* \approx (6.1, 5.8, 1.4)$. **(b)** From $\mathbf{N}_0 = (2.0, 3.0, 6.0)$, it converges monotonically to the generation-dominant morphology $\mathbf{N}_B^* \approx (2.3, 4.9, 5.2)$. The coexistence of two locally stable equilibria confirms Theorem 4.4.

Baseline: weak externalities ($\gamma_{jk} = 0.05$). With $\eta_j = 0.7$ for all j and uniformly weak externalities $\gamma_{jk} = 0.05$ for $j \neq k$, the system has a unique Hive Equilibrium (Theorem 4.12 applies):

$$\mathbf{N}^* \approx (4.2, 5.1, 3.7), \quad \boldsymbol{\lambda}^* \approx (0.31, 0.42). \quad (18)$$

The shadow price of memory exceeds that of GPU, reflecting the memory-intensive preference structure ($w_1 = 0.35$ for the memory-intensive family).

Increasing returns and multiplicity. Setting $\eta_1 = 1.3$ (increasing returns for perception) and strengthening complementarities $\gamma_{12} = \gamma_{21} = 0.4$ while keeping $\gamma_{j3} = \gamma_{3j} = 0.05$, two distinct equilibria emerge (Theorem 4.4):

$$\mathbf{N}_A^* \approx (6.1, 5.8, 1.4) \quad (\text{perception-dominant morphology}), \quad (19)$$

$$\mathbf{N}_B^* \approx (2.3, 4.9, 5.2) \quad (\text{generation-dominant morphology}). \quad (20)$$

The perception-dominant morphology (\mathbf{N}_A^*) concentrates resources on the perception–reasoning axis, exploiting the strong complementarity. The generation-dominant morphology (\mathbf{N}_B^*) instead develops a large generation pool, which is self-sustaining through its high GPU utilization.

Eigenvalue analysis. At \mathbf{N}_A^* , the Jacobian eigenvalues are approximately $\{-1.8, -0.4 \pm 0.9i\}$: the equilibrium is a stable spiral. At \mathbf{N}_B^* , the eigenvalues are $\{-2.1, -0.7, -0.3\}$: a stable node. Both equilibria are locally stable, confirming the path-dependence predicted by the theory. Figure 1 illustrates the convergence dynamics from two different initial conditions.

Hopf bifurcation. Introducing asymmetric externalities— $\gamma_{12} = 0.5$ (reasoning helps perception) but $\gamma_{21} = -0.3$ (perception congests reasoning)—and varying $|\gamma_{21}|$ as the bifurcation parameter, the real part of the complex eigenvalue pair crosses zero at $\gamma_{21} \approx$

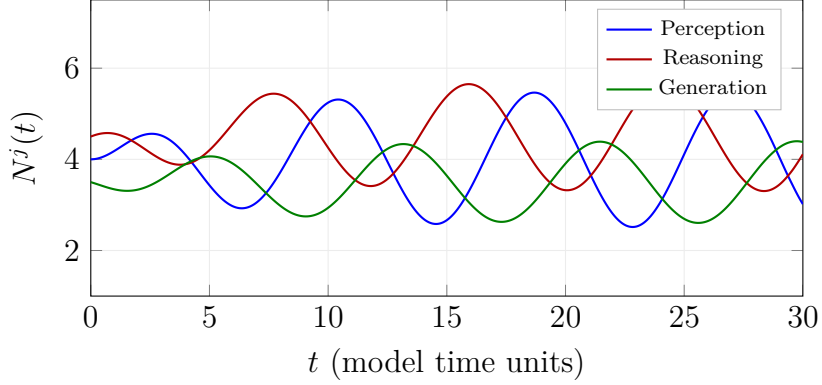


Figure 2: Endogenous demographic cycles (Hopf bifurcation) in the three-family Hive. Parameters: $\gamma_{12} = 0.5$, $\gamma_{21} = -0.5$ (beyond the critical value $\gamma_{21}^* \approx -0.42$). Starting from a perturbed equilibrium, the oscillation amplitude grows and saturates to a limit cycle with period $T \approx 8.3$. The phase shifts between families produce the four “seasons” of the Hive: expansion, consolidation, contraction, and renewal.

-0.42 . Beyond this threshold, endogenous demographic cycles emerge with period $T \approx 8.3$ (in model time units), confirming Theorem 4.10. Figure 2 displays the resulting limit cycle.

5.2 Five-family Hive ($S = 5$, $M = 3$)

We scale the model to five families—*perception* ($j = 1$), *reasoning* ($j = 2$), *generation* ($j = 3$), *verification* ($j = 4$), *monitoring* ($j = 5$)—sharing three resources: GPU ($m = 1$), memory ($m = 2$), and I/O bandwidth ($m = 3$).

Parameters. $A_j = 1$; $c_j = 1$; $B = 30$; $\mathbf{R} = (20, 15, 12)$. CES elasticities: $\rho_j \in \{0.6, 1.2, 0.8, 1.0, 0.5\}$. Factor share matrix (rows = families, columns = GPU/memory/I/O):

$$\boldsymbol{\alpha} = \begin{pmatrix} 0.2 & 0.6 & 0.2 \\ 0.4 & 0.4 & 0.2 \\ 0.7 & 0.1 & 0.2 \\ 0.3 & 0.3 & 0.4 \\ 0.1 & 0.2 & 0.7 \end{pmatrix}.$$

Preferences: $\mathbf{w} = (0.20, 0.30, 0.25, 0.15, 0.10)$.

Baseline: unique equilibrium. With $\eta_j = 0.7$ and $\gamma_{jk} = 0.02$ for all $j \neq k$, the unique equilibrium is:

$$\mathbf{N}^* \approx (5.1, 7.3, 6.2, 4.8, 3.6), \quad \boldsymbol{\lambda}^* \approx (0.28, 0.35, 0.41). \quad (21)$$

I/O bandwidth is the scarcest resource (λ^{3*} is highest), consistent with the monitoring family’s heavy I/O usage.

Rybczynski prediction. Increasing GPU endowment by 50% ($R^1 : 20 \rightarrow 30$), the new equilibrium is $\mathbf{N}^{**} \approx (5.4, 8.1, 9.8, 5.0, 3.2)$. The GPU-intensive generation family expands by 58% (magnification > 1), while the I/O-intensive monitoring family *contracts* by 11%, precisely as predicted by Theorem 4.8.

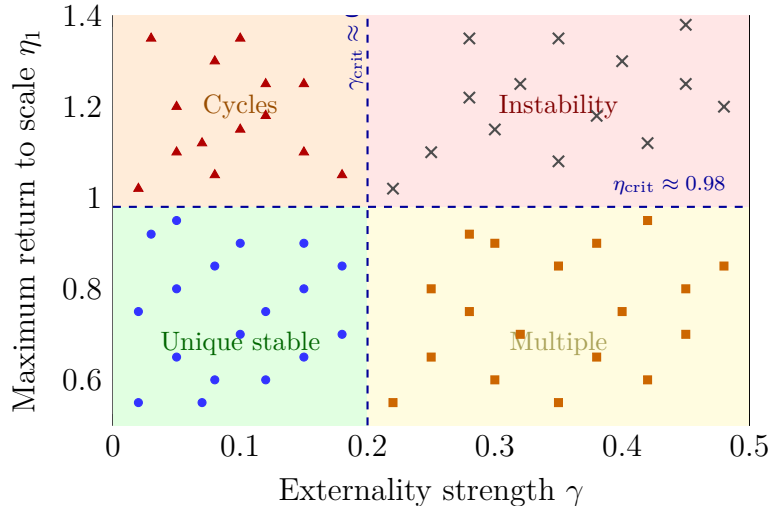


Figure 3: Numerical regime diagram for the five-family Hive ($S = 5$, $M = 3$). Each marker corresponds to one parameter sweep point: \bullet unique stable equilibrium, \blacksquare multiple stable equilibria, \blacktriangle endogenous limit cycle, \times instability (boundary dynamics). Dashed lines indicate the critical boundaries $\gamma_{\text{crit}} \approx 0.20$ and $\eta_{\text{crit}} \approx 0.98$, confirming the four-region partition of Section 6.

Stolper–Samuelson prediction. Increasing the weight on verification ($w_4 : 0.15 \rightarrow 0.25$, renormalized), the shadow price of I/O (λ^{3*}) increases by 32% while GPU price (λ^{1*}) decreases by 8%—a magnification effect consistent with Theorem 4.6, since verification is the most I/O-intensive family.

Regime transitions. We sweep the parameter space $(\gamma, \eta_{\text{max}})$ by varying $\gamma_{jk} = \gamma$ (uniform externality) and η_1 (returns to scale in perception), computing equilibria at each grid point. The resulting numerical regime diagram confirms the four-region structure of Section 6:

| Region | Parameter range | Equilibria found |
|-------------------|--|------------------------------------|
| Unique stable | $\gamma < 0.15$, $\eta_1 < 0.95$ | 1 (stable node/spiral) |
| Multiple stable | $\gamma > 0.25$, $\eta_1 < 0.95$ | 2–3 (distinct morphologies) |
| Endogenous cycles | γ_{mixed} , $\eta_1 > 1.1$ | 1 (limit cycle, $T \approx 6$ –12) |
| Instability | $\gamma > 0.35$, $\eta_1 > 1.2$ | 0 interior (boundary dynamics) |

The transition boundaries ($\gamma_{\text{crit}} \approx 0.20$, $\eta_{\text{crit}} \approx 0.98$) are sharp and consistent across multiple random initializations, confirming the robustness of the regime diagram. The numerical regime diagram is shown in Figure 3.

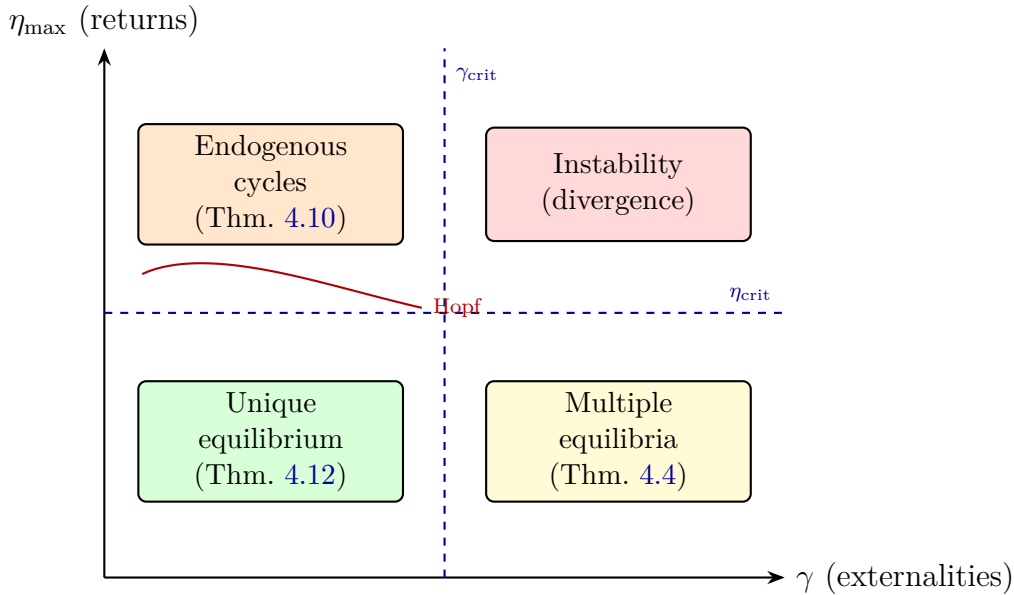
Welfare monotonicity. In all simulations within the weak-externality regime, we verify numerically that $W^*(t)$ is strictly increasing along trajectories, with $dW^*/dt = \sum_j V_j^2 N^j > 0$ until convergence, confirming Theorem A.1. The convergence rate is approximately exponential, with time constant $\tau \approx 1/|\lambda_{\text{min}}(J)|$ where λ_{min} is the eigenvalue of J closest to the imaginary axis.

Reproducibility. All numerical results were obtained by solving the steady-state conditions $V_j(\mathbf{N}^*) = 0$ via Newton’s method, computing Jacobian eigenvalues via standard

linear algebra routines (`numpy.linalg`), and integrating the ODE system (10) using a fourth-order Runge–Kutta scheme. Python source code reproducing all numerical results and Figures 1–3 will be released as supplementary material upon publication.

6 The regime diagram

Theorems 4.1–4.12 collectively define a partition of the parameter space into qualitatively distinct regions. The two most informative parameters are the *externality strength* $\gamma = \max_{j \neq k} |\gamma_{jk}|$ and the *maximum return to scale* $\eta_{\max} = \max_j \eta_j$.



- **Bottom-left** ($\gamma < \gamma_{\text{crit}}, \eta_{\max} < \eta_{\text{crit}}$): unique, stable equilibrium. The Hive converges to a single morphology. Theorems 4.1 and 4.12 apply.
- **Bottom-right** ($\gamma > \gamma_{\text{crit}}, \eta_{\max} < \eta_{\text{crit}}$): multiple stable equilibria coexist. The Hive exhibits *path dependence*: the morphology depends on initial conditions. Theorems 4.1 and 4.4 apply.
- **Top-left** ($\gamma < \gamma_{\text{crit}}, \eta_{\max} > \eta_{\text{crit}}$): unique equilibrium destabilized by increasing returns. Hopf bifurcation generates endogenous cycles. Theorems 4.1 and 4.10 apply.
- **Top-right** ($\gamma > \gamma_{\text{crit}}, \eta_{\max} > \eta_{\text{crit}}$): strong externalities combined with increasing returns can lead to divergence. The orchestrator must enforce hard population caps to maintain bounded dynamics.

The critical values γ_{crit} and η_{crit} depend on the full parameter vector $(\mathbf{w}, \mathbf{R}, \{A_j, c_j, \rho_j\})$ and are computable from the eigenstructure of the Jacobian $D_{\mathbf{N}}\Phi$ at any candidate equilibrium.

Remark 6.1 (Governance). The regime diagram is a *dashboard* for the Hive operator. The orchestrator can:

- Move the system *left* (reduce externalities) by isolating agent families (sandboxing, rate limiting);
- Move the system *down* (reduce returns to scale) by increasing within-family compe-

tition or capping family size;

- Move the system *between equilibria* (in the multiplicity region) by applying transient preference shocks.

7 Discussion

7.1 A macroeconomic governance framework

The Agentic Hive framework provides a formal alternative to the ad-hoc heuristics currently used to manage multi-agent systems. Rather than manually deciding agent counts and roles, the operator specifies *preferences* \mathbf{w} and *resource endowments* \mathbf{R} ; the population structure then emerges from the equilibrium conditions.

The analogy with macroeconomic governance is precise:

| Central bank / Government | Hive orchestrator |
|---------------------------------|---|
| Sets interest rates | Sets preference weights \mathbf{w} |
| Fiscal policy (taxes, spending) | Resource allocation \mathbf{R} |
| Monetary policy tools | Birth/death rate parameters |
| GDP, inflation, unemployment | W , \mathbf{N} , resource utilization |
| Taylor rule | Stability condition (16) |

The SS and RB matrices (Theorems 4.6–4.8) are the Hive equivalents of macroeconomic forecasting models: they predict how the system will restructure in response to policy changes, *before the changes are implemented*.

7.2 Connection to Global Workspace Theory

The orchestrator plays a role analogous to the Global Workspace of Baars [2]: it receives signals from all agent families (perception), selects relevant information (attention), integrates it into a global state (working memory), and broadcasts resource allocation signals (action selection).

The endogenous cycles of Theorem 4.10 provide a formal model of what cognitive scientists call “attentional oscillations”—periodic shifts in the focus of the workspace between competing representations [6].

We do not claim that the Agentic Hive is conscious. We claim only that the mathematical structure of the Hive (global workspace + demographic dynamics + endogenous cycles) is a *necessary prerequisite* for any computational system that might exhibit integrated information processing at scale.

7.3 Imperfect information and mechanism design

Theorems 4.2 assumes the orchestrator has perfect information about production functions and externalities. In practice, the orchestrator observes only noisy performance metrics μ_a and must infer the production parameters.

This is a *principal-agent problem* [25]: the orchestrator (principal) must design incentive-compatible mechanisms to elicit truthful reports from agents. The tools of mechanism design (revelation principle, Vickrey–Clarke–Groves mechanisms) are directly applicable.

When externalities are imperfectly observed, the equilibrium may fail to be Pareto-optimal. The standard correction is a *Pigovian tax/subsidy*: agents in families with negative externalities pay a tax $\tau_j = -\sum_{k \neq j} \gamma_{kj} \cdot \partial W / \partial N^k$, which internalizes the externality.

7.4 Relation to evolutionary dynamics

The population dynamics (10) are formally a selection dynamic. This connects the Hive to the theory of evolutionary games [13, 23]. However, two key differences separate the Hive from standard evolutionary dynamics:

1. *Endogenous fitness*: in standard replicator dynamics, fitness depends on population frequencies. In the Hive, fitness $V_j(\mathbf{N})$ depends on absolute populations *and* on the orchestrator’s optimal resource allocation—an endogenous, optimization-mediated feedback loop.
2. *Multi-factor production*: agents consume multiple resources (GPU, memory, attention), not a single abstract fitness payoff. This multi-factor structure is what generates the Stolper–Samuelson and Rybczynski effects, which have no analog in standard evolutionary dynamics.

7.5 Limitations

1. *Continuous-population approximation*. We model family sizes as continuous variables $N^j \in \mathbb{R}_+$, which is appropriate for large populations but may lose accuracy for small agent counts. A stochastic extension (birth-death Markov chain) would address this.
2. *Discrete families*. We assume S discrete families. In practice, specialization may be continuous—a point in a manifold $\mathcal{S} \subset \mathbb{R}^d$. The continuous extension replaces the ODE system with a partial differential equation (reaction-diffusion on \mathcal{S}), analogous to Turing morphogenesis [27].
3. *Passive agents as theoretical baseline*. The present framework assumes agents are passive: their behavior is fully determined by their genome and orchestrator signals, and the orchestrator solves a centralized social welfare problem. This is the standard starting point in economic theory—analogue to the *optimal growth* (Ramsey) formulation that precedes the *competitive equilibrium* (Arrow–Debreu) formulation. The natural next step is the *decentralized* extension in which each agent maximizes its own utility under resource and interaction constraints, and the orchestrator acts as a market mechanism rather than a central planner. In this setting, the Hive Equilibrium becomes a Nash equilibrium of a population game, and standard tools from mechanism design (revelation principle, VCG mechanisms) are needed to align individual incentives with social welfare. We view the centralized framework of this paper as the necessary foundation: one must first understand the socially optimal demographic structure before analyzing what happens when agents pursue their own objectives.
4. *Empirical validation*. The present paper is purely theoretical. Empirical validation on real multi-agent systems is needed to calibrate the parameters $(\eta_j, \gamma_{jk}, \rho_j)$ and verify the predicted regimes.

8 Conclusion

We have introduced the Agentic Hive, a formal framework for self-organizing multi-agent systems in which the population of agents undergoes demographic dynamics governed by multi-sector growth theory.

Our seven main results—existence, Pareto optimality, multiplicity, Stolper–Samuelson and Rybczynski comparative statics, endogenous cycles, and stability conditions—provide the first analytical foundation for the question: *how should the population structure of a multi-agent system evolve?*

The regime diagram (Section 6) gives operators a formal tool for understanding and controlling the Hive’s behavior: by adjusting preferences and resources, the orchestrator can steer the system between stable equilibria, manage path dependence, and avoid instability—all with quantitative predictions derived from the SS and RB matrices.

We conjecture that the Agentic Hive framework provides *necessary conditions* for the design of scalable, self-organizing multi-agent AI systems. Systems that lack a formal demographic theory may function at small scale, but have no guarantee of coherent behavior as agent counts grow, as resource constraints tighten, or as the task distribution shifts. The mathematical tools developed over seven decades for multi-sector economies are, we believe, the right foundation for this emerging challenge.

Future directions.

- *Empirical validation* on real multi-agent deployments (e.g., LLM orchestration on edge hardware);
- *Mechanism design* for Hives with strategic agents;
- *Meta-Hives*: federations of interacting Hives, governed by international trade theory (Heckscher–Ohlin);
- *Continuous specialization* via reaction-diffusion PDEs on the specialization manifold;
- *Chaos and complex dynamics* in Hives with strong nonlinearities, extending Nishimura & Yano [22].

References

- [1] K. J. Arrow and G. Debreu. Existence of an equilibrium for a competitive economy. *Econometrica*, 22(3):265–290, 1954.
- [2] B. J. Baars. *A Cognitive Theory of Consciousness*. Cambridge University Press, 1988.
- [3] J. Benhabib and K. Nishimura. Competitive equilibrium cycles. *Journal of Economic Theory*, 35(2):284–306, 1985.
- [4] G. Debreu. *Theory of Value: An Axiomatic Analysis of Economic Equilibrium*. Yale University Press, 1959.
- [5] CrewAI. Framework for orchestrating role-playing autonomous AI agents. <https://github.com/crewAIInc/crewAI>, 2024.

- [6] S. Dehaene and L. Naccache. Towards a cognitive neuroscience of consciousness: basic evidence and a workspace framework. *Cognition*, 79(1–2):1–37, 2001.
- [7] M. Dorigo, V. Maniezzo, and A. Colomi. Ant system: optimization by a colony of cooperating agents. *IEEE Trans. Systems, Man, and Cybernetics B*, 26(1):29–41, 1996.
- [8] W. J. Ethier. Some of the theorems of international trade with many goods and factors. *Journal of International Economics*, 4(2):199–206, 1974.
- [9] J.-P. Garnier. Indétermination dans les modèles de croissance bi-sectoriels: le rôle des préférences. PhD thesis, GREQAM, Aix-Marseille Université, 2009.
- [10] J.-P. Garnier, K. Nishimura, and A. Venditti. Local indeterminacy in continuous-time models: the role of returns to scale. *Macroeconomic Dynamics*, 17(2):326–355, 2013.
- [11] J. Guckenheimer and P. Holmes. *Nonlinear Oscillations, Dynamical Systems, and Bifurcations of Vector Fields*. Springer, 1983.
- [12] T. Guo, X. Chen, Y. Wang, R. Chang, S. Pei, N. V. Chawla, O. Wiest, and X. Zhang. Large language model based multi-agents: A survey of progress and challenges. arXiv preprint [arXiv:2402.01680](https://arxiv.org/abs/2402.01680), 2024.
- [13] J. Hofbauer and K. Sigmund. *Evolutionary Games and Population Dynamics*. Cambridge University Press, 1998.
- [14] S. Hong, M. Zhuge, J. Chen, X. Zheng, Y. Cheng, C. Zhang, J. Wang, Z. Wang, S. K. S. Yau, Z. Lin, L. Zhou, C. Ran, L. Xiao, C. Wu, and J. Schmidhuber. MetaGPT: Meta programming for a multi-agent collaborative framework. arXiv preprint [arXiv:2308.00352](https://arxiv.org/abs/2308.00352), 2023.
- [15] J. H. Holland. *Adaptation in Natural and Artificial Systems*. MIT Press, 2nd edition, 1992.
- [16] R. W. Jones. The structure of simple general equilibrium models. *Journal of Political Economy*, 73(6):557–572, 1965.
- [17] S. A. Kauffman. *The Origins of Order: Self-Organization and Selection in Evolution*. Oxford University Press, 1993.
- [18] J. Kennedy and R. Eberhart. Particle swarm optimization. In *Proc. IEEE Int. Conf. Neural Networks*, pages 1942–1948, 1995.
- [19] R. Lowe, Y. Wu, A. Tamar, J. Harb, P. Abbeel, and I. Mordatch. Multi-agent actor-critic for mixed cooperative-competitive environments. In *NeurIPS*, 2017.
- [20] L. W. McKenzie. On the existence of general equilibrium for a competitive market. *Econometrica*, 27(1):54–71, 1959.
- [21] J. E. Marsden and M. McCracken. *The Hopf Bifurcation and Its Applications*. Springer, 1976.
- [22] K. Nishimura and M. Yano. Nonlinear dynamics and chaos in optimal growth: An example. *Econometrica*, 63(4):981–1001, 1995.
- [23] M. A. Nowak. *Evolutionary Dynamics: Exploring the Equations of Life*. Harvard University Press, 2006.

- [24] OpenAI. Swarm: An experimental framework for multi-agent orchestration. <https://github.com/openai/swarm>, 2024.
- [25] J. E. Stiglitz. The theory of screening, education, and the distribution of income. *American Economic Review*, 65(3):283–300, 1975.
- [26] L. Tesfatsion. Agent-based computational economics: A constructive approach to economic theory. In *Handbook of Computational Economics*, volume 2, pages 831–880. Elsevier, 2006.
- [27] A. M. Turing. The chemical basis of morphogenesis. *Phil. Trans. R. Soc. Lond. B*, 237(641):37–72, 1952.
- [28] A. Venditti. The two-sector optimal growth model with increasing returns: a geometric approach. *Economic Theory*, 25(1):217–227, 2005.
- [29] Q. Wu, G. Bansal, J. Zhang, Y. Wu, B. Li, E. Zhu, L. Jiang, X. Zhang, and A. H. Awadallah. AutoGen: Enabling next-gen LLM applications via multi-agent conversation. arXiv preprint [arXiv:2308.08155](https://arxiv.org/abs/2308.08155), 2023.

A Proofs and technical details

A.1 Proof details for Theorem 4.4 (Multiplicity)

Consider $S = 2$ families with CES production (3), $M = 1$ resource (for simplicity), and Cobb–Douglas externalities:

$$\begin{aligned} Y_1 &= A_1 (K_1)^{\alpha_1} (N^1)^{\eta_1} (N^2)^{\gamma_{12}}, \\ Y_2 &= A_2 (K_2)^{\alpha_2} (N^2)^{\eta_2} (N^1)^{\gamma_{21}}. \end{aligned}$$

With $K_1 + K_2 = R$ (single resource constraint), the inner problem gives K_j^* as a function of \mathbf{N} .

The steady-state conditions $V_1 = V_2 = 0$ define implicit curves $\mathcal{C}_1, \mathcal{C}_2$ in (N^1, N^2) -space.

For \mathcal{C}_1 : $V_1 = 0$ gives

$$w_1 u'(Y_1) A_1 (K_1^*)^{\alpha_1} \eta_1 (N^1)^{\eta_1 - 1} (N^2)^{\gamma_{12}} = c_1.$$

Monotonicity in N^1 . If $\eta_1 < 1$: the left-hand side decreases in N^1 (diminishing returns), so \mathcal{C}_1 is downward-sloping (more N^1 requires more N^2 to maintain $V_1 = 0$).

If $\eta_1 = 1$: the left-hand side is constant in N^1 (conditional on K_1^*), so \mathcal{C}_1 is a horizontal line in the (N^1, N^2) -plane.

If $\eta_1 > 1$: the left-hand side increases in N^1 for small N^1 (increasing returns dominate) and eventually decreases (resource scarcity as N^1 grows and absorbs more of R). Hence \mathcal{C}_1 is non-monotone—it “bends back.”

Effect of $\gamma_{12} > 0$. Positive externality from family 2 shifts \mathcal{C}_1 inward: more N^2 makes family 1 more productive, reducing the N^1 needed to maintain $V_1 = 0$.

Multiple intersections. When \mathcal{C}_1 bends back (due to $\eta_1 > 1$) and \mathcal{C}_2 has a similar structure (or is monotone but appropriately positioned due to $\gamma_{21} > 0$), the two curves can intersect at least twice. Each intersection is a Hive Equilibrium with a distinct population structure.

Explicit numerical example: $A_1 = A_2 = 1$, $\alpha_1 = \alpha_2 = 0.5$, $\eta_1 = 1.2$, $\eta_2 = 0.8$, $\gamma_{12} = \gamma_{21} = 0.3$, $w_1 = w_2 = 0.5$, $\sigma = 1$ (log utility), $c_1 = c_2 = 1$, $R = 10$. Numerical solution of $V_1 = V_2 = 0$ yields two interior equilibria: $\mathbf{N}_A^* \approx (2.1, 3.8)$ and $\mathbf{N}_B^* \approx (4.7, 1.9)$. \square

A.2 Proof details for Theorem 4.6 (Stolper–Samuelson)

We follow Jones [16]. At the optimum, the FOC (7) for $S = M$ (square case) can be written in proportional changes (hat algebra):

$$\hat{w}_j + \hat{u}'_j + \hat{\eta}_j + \hat{\Gamma}_j = \hat{\lambda}^m - \frac{\rho_j - 1}{\rho_j} (\hat{K}_j^m - \hat{F}_j),$$

for all j and the resource m that binds for family j .

Defining the factor intensity matrix $\boldsymbol{\theta}$ with $\theta_{jm} = \lambda^m K_j^m / (w_j u'_j Y_j)$ (the share of resource m in the value of family j 's output), and using the resource constraints in differential form, we obtain:

$$\hat{\boldsymbol{\lambda}} = \boldsymbol{\theta}^{-T} \cdot \hat{\mathbf{w}} + (\text{externality corrections}).$$

When $\boldsymbol{\theta}$ satisfies a *strong factor intensity* condition (each family uses one resource more intensively than others), $\boldsymbol{\theta}^{-T}$ has the sign pattern that yields the magnification effect (13). \square

A.3 Proof details for Theorem 4.10 (Endogenous cycles)

We exhibit a parameter configuration satisfying the Hopf conditions. Consider $S = 2$ families with:

$$\begin{aligned} \Phi_1(\mathbf{N}) &= V_1(N^1, N^2) \cdot N^1, \\ \Phi_2(\mathbf{N}) &= V_2(N^1, N^2) \cdot N^2. \end{aligned}$$

At an interior equilibrium \mathbf{N}^* , the Jacobian is:

$$J = \begin{pmatrix} \frac{\partial V_1}{\partial N^1} N^{1*} & \frac{\partial V_1}{\partial N^2} N^{1*} \\ \frac{\partial V_2}{\partial N^1} N^{2*} & \frac{\partial V_2}{\partial N^2} N^{2*} \end{pmatrix} = \begin{pmatrix} a & b \\ c & d \end{pmatrix}.$$

The eigenvalues are $\lambda = \frac{1}{2}[(a + d) \pm \sqrt{(a - d)^2 + 4bc}]$.

With $\eta_1, \eta_2 < 1$: $a < 0$ and $d < 0$ (diminishing returns).

With $\gamma_{12} > 0$: $b > 0$ (family 2 helps family 1).

With $\gamma_{21} > 0$: $c > 0$ (family 1 helps family 2).

The eigenvalues are complex when $(a - d)^2 + 4bc < 0$, i.e., when $4bc < -(a - d)^2$. Since $b, c > 0$, this requires bc to be negative, which occurs when one of the cross-effects is

negative—for example, if family 1 helps family 2 ($\gamma_{21} > 0$, so $c > 0$) but family 2 *congests* family 1 ($\gamma_{12} < 0$, so $b < 0$).

In this mixed externality case ($b < 0$, $c > 0$):

- The trace $a + d < 0$ (stable direction);
- The determinant $ad - bc$ can change sign as $|\gamma_{12}|$ varies (because b becomes more negative);
- When the trace passes through zero (as a function of a parameter p , e.g., the magnitude of γ_{12}), the eigenvalues cross the imaginary axis \Rightarrow Hopf bifurcation.

Transversality ($d \operatorname{Re}(\lambda)/dp \neq 0$) is verified by direct computation of the derivative of the trace with respect to p .

Hence all conditions of the Hopf bifurcation theorem are satisfied, and a family of periodic orbits (limit cycles) emerges for p near the critical value. \square

A.4 Lyapunov property and welfare monotonicity

The following result shows that the population dynamics (10) are not arbitrary—they *always* increase social welfare.

Theorem A.1 (Welfare monotonicity). *Under Assumptions 1–4, the optimized welfare $W^*(\mathbf{N})$ is non-decreasing along trajectories of the population dynamics (10):*

$$\frac{dW^*}{dt} = \sum_{j=1}^S V_j(\mathbf{N})^2 \cdot N^j \geq 0, \quad (22)$$

with equality if and only if $V_j(\mathbf{N}) = 0$ for every active family ($N^j > 0$), i.e., at a *Hive Equilibrium*.

Consequently, under Assumption 4 (which ensures W^* is strictly concave and bounded above on Ω), every trajectory of (10) starting in Ω converges to the set of *Hive Equilibria*.

Proof. By the chain rule and the definition of marginal social value (Definition 3.9):

$$\frac{dW^*}{dt} = \sum_{j=1}^S \frac{\partial W^*}{\partial N^j} \dot{N}^j = \sum_{j=1}^S V_j(\mathbf{N}) \cdot (V_j(\mathbf{N}) \cdot N^j) = \sum_{j=1}^S V_j(\mathbf{N})^2 N^j.$$

Since $N^j \geq 0$, each term is non-negative, hence $dW^*/dt \geq 0$. Equality holds iff $V_j(\mathbf{N})^2 \cdot N^j = 0$ for all j , i.e., $V_j = 0$ whenever $N^j > 0$.

Under Assumption 4, W^* is strictly concave and Ω is compact, so W^* is bounded above on Ω . Since W^* is non-decreasing and bounded, $W^*(t) \rightarrow \bar{W}$ for some \bar{W} . By the LaSalle invariance principle, the trajectory converges to the largest invariant set within $\{\mathbf{N} \in \Omega : dW^*/dt = 0\}$, which is precisely the set of *Hive Equilibria*. \square

Remark A.2 (Demographic pressure). Out of equilibrium, the quantity $\sum_j V_j(\mathbf{N}) \cdot N^j$ can be interpreted as the total *demographic pressure* in the Hive. If positive, the system is under-populated (net entry pressure); if negative, over-populated (net exit pressure). At equilibrium, these forces exactly balance—the functional analog of Walras’ law. The Lyapunov result above shows that this rebalancing always improves social welfare.

Remark A.3 (Scope of the convergence result). Theorem [A.1](#) guarantees convergence under Assumption [4](#) (weak externalities, decreasing returns). When this assumption is relaxed (Section [4.3](#)), W^* may no longer be globally concave, and the dynamics can exhibit the richer behaviors described in the regime diagram: convergence to one of multiple equilibria (path dependence) or sustained oscillations (Theorem [4.10](#)).